

Pre-Supernova Evolution of Massive Stars

By NINO PANAGIA^{1,2}, AND GIUSEPPE BONO³

¹Space Telescope Science Institute, 3700 San Martin Drive, Baltimore, MD 21218, USA.

²On assignment from the Space Science Department of ESA.

³Osservatorio Astronomico di Roma, Via Frascati 33, Monte Porzio Catone, Italy.

We present the preliminary results of a detailed theoretical investigation on the hydrodynamical properties of Red Supergiant (RSG) stars at solar chemical composition and for stellar masses ranging from 10 to 20 M_{\odot} . We find that the main parameter governing their hydrodynamical behaviour is the effective temperature, and indeed when moving from higher to lower effective temperatures the models show an increase in the dynamical perturbations. Also, we find that RSGs are pulsationally unstable for a substantial portion of their lifetimes. These dynamical instabilities play a key role in driving mass loss, thus inducing high mass loss rates (up to almost $10^{-3} M_{\odot} yr^{-1}$) and considerable variations of the mass loss activity over timescales of the order of 10^4 years. Our results are able to account for the variable mass loss rates as implied by radio observations of type II supernovae, and we anticipate that comparisons of model predictions with observed circumstellar phenomena around SNII will provide valuable diagnostics about their progenitors and their evolutionary histories.

1. Introduction

More than 20 years of radio observations of supernovae (SNe) have provided a wealth of evidence for the presence of substantial amounts of circumstellar material (CSM) surrounding the progenitors of SNe of type II and Ib/c (see Weiler *et al.*, this Conference, and references therein). Also, the radio measurements indicate that (a) the CSM density falls off like r^{-2} , suggesting a constant velocity, steady wind, and that (b) the density is so high as to require a ratio of the mass loss rate, \dot{M} , to the wind velocity, w , to be higher than $\dot{M}/w \sim 10^{-7} M_{\odot} yr^{-1} km s^{-1}$. These requirements are best satisfied by red supergiants (RSG), with original masses in the range 8-30 M_{\odot} , that indeed are the putative progenitors of SNII. Note that in the case of SNe Ib/c, the stellar progenitor cannot provide such a dense CSM directly and that a wind from a binary companion must be invoked to explain the observations (Panagia and Laidler 1988, Boffi and Panagia 1996, 2000).

This scenario is able to account for the basic properties of all radio SNe. However, the evolution of SN 1993J indicated that the progenitor mass loss rate had declined by almost a factor of 10 in the last few thousand years before explosion (Van Dyk *et al.* 1994). In addition, there are SNe, such as SN 1979C (Montes *et al.* 2000), SN 1980K (Montes *et al.* 1998), and SN 1988Z (Lacey *et al.* 2000), that have displayed relatively sudden changes in their radio emission evolution about 10 years after explosion, which also cannot be explained in term of a constant mass loss rate. Since a SN shock front, where the radio emission originates, is moving at about $10,000 km s^{-1}$ and a RSG wind is typically expanding at $10 km s^{-1}$, a sudden change in the CSM density about ten years after explosion implies a relatively quick change of the RSG mass loss rate about 10,000 years before it underwent the SN explosion. These findings are summarized in Figure 1 that, for several well studied RSNe, displays the mass loss rate implied by radio observations as a function of the look-back time, calculated simply as the actual time since explosion multiplied by a factor of 1000, which is the ratio of the SN shock velocity to the RSG wind velocity.

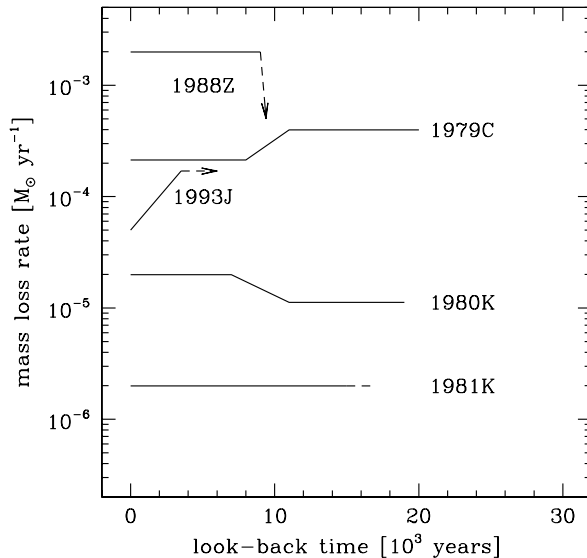


FIGURE 1. Mass loss rates as a function of look-back time as measured for a number radio supernovae (adapted from Weiler *et al.* 2000; schematic)

Additional evidence for enhanced mass loss from SNII progenitors over time intervals of several thousand years is provided also by the detection of relatively narrow emission lines with typical widths of several 100 km s^{-1} in the spectra of a number of SNII (e.g. SN 1978K: Ryder *et al.* 1993, Chugai, Danziger & Della Valle 1995, Chu *et al.* 1999; SN 1997ab: Salamanca *et al.* 1998; SN 1996L: Benetti *et al.* 1999), that indicate the presence of dense circumstellar shells ejected by the SN progenitors in addition to a more diffuse, steady wind activity.

We note that a time of about 10,000 years is a sizeable fraction of the time spent by a massive star in the RSG phases and implies a kind of variability which is not predicted by standard stellar evolution. In particular, a time scale of $\sim 10^4$ years is considerably shorter than the H and He burning phases but is much longer than any of the successive nuclear burning phases that a massive star goes through before core collapse (e.g. Chieffi *et al.* 1999). Therefore, some other phenomenon is to be sought to properly account for the observations.

Another problem which needs to be addressed is the actual rate of mass loss for red supergiants. The observational evidence is that mass loss rates in the range 10^{-6} – $10^{-4} M_{\odot} \text{ yr}^{-1}$ are commonly found in RSG, with a relatively steep increase in mass loss activity for the coolest stars (e.g. Reid, Tinney & Mould 1990, Feast 1991). On the other hand, there is no satisfactory theory to predict mass loss rates in these phases of stellar evolution, and current parametrizations fall short from describing the phenomenon in detail. For example, let us consider the classical formula by Reimers (1975),

$$\log(\dot{M}) = -12.6 + \log\left(\frac{LR}{GM}\right) + \log(\eta)$$

which can be rewritten as:

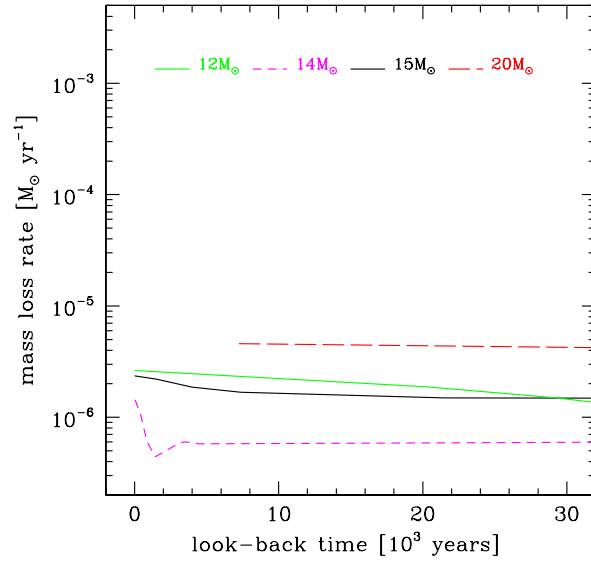


FIGURE 2. Mass loss rates predicted from canonical stellar evolution theory by using Reimers' formula.

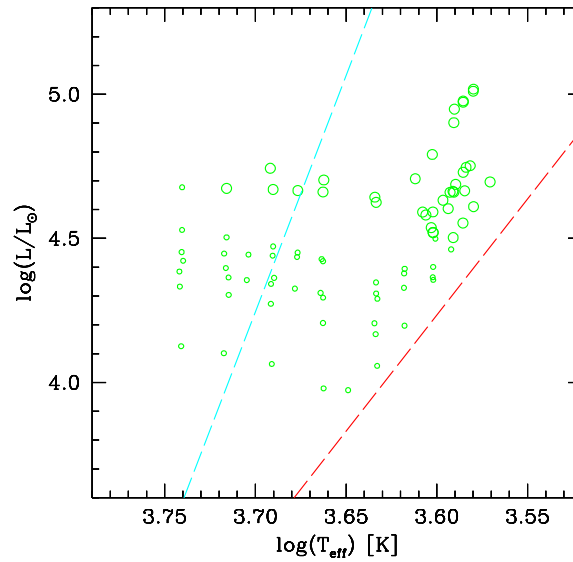


FIGURE 3. Predicted mass loss rates as a function of the position in the HR diagram adopting Reimers' formula. The size of the circles are proportional to the logarithm of the mass loss rate: the highest values are several $10^{-6} M_{\odot} yr^{-1}$ and the lowest ones about $10^{-7} M_{\odot} yr^{-1}$. The dashed lines represent the analytical relations for the fundamental blue and red edges of the Cepheid instability strip defined by Bono *et al.* (2000a).

$$\dot{M} \propto \eta \frac{L^{1.5}}{M T_{eff}^2}$$

This formula was devised to dimensionally account for the mass loss from low-mass red giants, but has also been widely adopted for evolutionary track calculations. We see that the predicted mass loss rate varies rather slowly when a star is moving from the blue to the red region (i.e. during H-shell burning and/or He-core burning) of the HR diagram, the main functional dependence being a 1.5 power of the luminosity. The corresponding mass loss rates, computed using the evolutionary tracks by Bono *et al.* (2000b) for stars in the mass range $10\text{--}20M_{\odot}$, are shown in Figures 2 and 3. It is apparent that not only the rates are not as high as suggested by spectroscopic observations of RSGs (this aspect alone could easily be "fixed" by increasing the efficiency factor η) but, more importantly, are very slowly varying with time and, therefore, cannot account for radio observations of SNe, either.

Other parametrizations of the mass loss rate in the HR diagram have been proposed by different authors (e.g. De Jager, Nieuwenhuijzen & van der Hucht 1988, Salasnich, Bressan and Chiosi 1999), but insofar for RSGs the main dependence of \dot{M} is a power of ~ 2 of the luminosity, they all are unable to reproduce appreciable mass loss variations over a timescale of roughly 10^4 years.

Actually, one notices that for masses above $10 M_{\odot}$, the last phases of the RGS evolution fall within the extrapolation of the Cepheid instability strip (see Figure 4), as calculated by Bono *et al.* (1996), and therefore, one may expect that pulsational instabilities could represent the additional mechanism needed to trigger high mass loss rates. Indeed, the pioneering work of Heber *et al.* (1997), based on both linear and nonlinear pulsation models, demonstrated that RSG stars are pulsationally unstable. In particular, they found that, for periods approaching the Kelvin-Helmoltz time scale, these stars display large luminosity amplitudes, which could trigger a strong enhancement in their mass loss rate before they explode as supernovae. According to these authors this pulsation behaviour should take place during the last few 10^4 yrs before the core collapse, due to the large increase in the luminosity to mass ratio experienced by RSG stars during these evolutionary phases.

However, the nonlinear calculations performed by Heber *et al.* (1997) were hampered by the fact that their hydrodynamic code could not properly handle pulsation destabilizations characterized both by small growth rates due to numerical damping, and by large pulsation amplitudes due to the formation and propagation of strong shock waves during the approach to limit cycle stability. Also, as Heber *et al.* (1997) pointed out, their main theoretical difficulty in dealing with the dynamical instabilities of RSG variables resided in the coupling between convection and pulsation. In fact, they constructed the linear models by assuming that the convective flux is frozen in, and the nonlinear ones by assuming that the convective flux is instantaneously adjusted. However, this treatment does not account for the driving and/or quenching effects caused by the interaction between pulsation and convection: this shortcoming may explain why their nonlinear models could not approach a stable limit cycle.

It is clear that a more general approach must be adopted to solve the problem. This motivated us to start a systematic study of the pulsational properties of massive stars. In the following we shall illustrate briefly the procedures adopted and the first results obtained (Section 2), and will present and discuss our findings on the mass loss rates in the late phases of the evolution of massive stars (Sections 3 and 4).

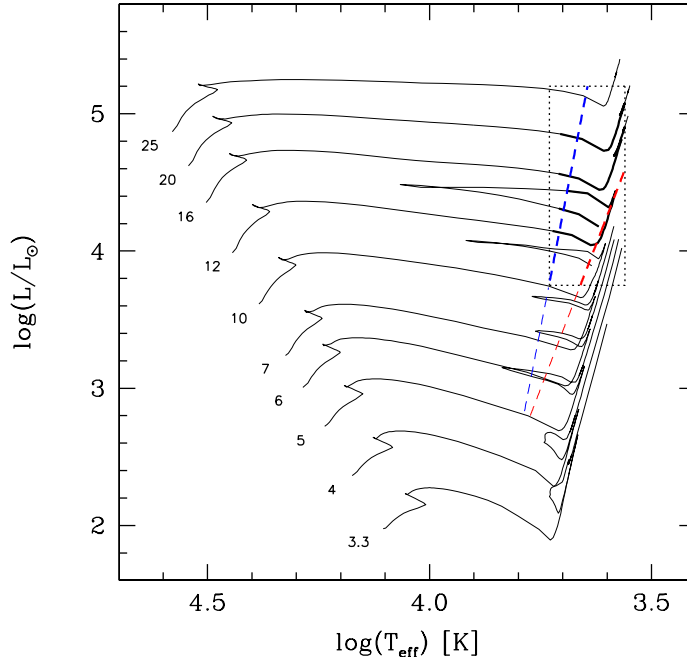


FIGURE 4. Evolutionary tracks for stars in the range $3.3\text{--}25 M_{\odot}$. The marked area is the portion of the HR diagram shown in more detail in Figure 5. The dashed lines are the extrapolation of the fundamental boundaries of the Cepheid instability strip according to the analytical relations provided by Bono *et al.* (2000a), which are based on a detailed investigation of Cepheid models at solar chemical composition and stellar masses ranging from 5 to $11 M_{\odot}$. Note that a substantial portion of both H-shell and He burning phases for stars with masses higher than about $10 M_{\odot}$ occur within the instability strip.

2. Theoretical Framework

The procedures employed to construct both linear and nonlinear models of high-mass radial variables have been described in detail in a number of papers (Bono & Stellingwerf 1994; Bono, Caputo, & Marconi 1998; Bono, Marconi & Stellingwerf 1999), so that a brief outline of the methods adopted will suffice here. In particular:

- We constructed a set of limiting amplitude, nonlinear, convective models of Red Super Giant (RSG) variables during both hydrogen and helium burning evolutionary phases.
- A Lagrangian one-dimensional hydrocode was used in which local conservation equations are simultaneously solved with a nonlocal, time-dependent convective transport equation (Stellingwerf 1982; Bono & Stellingwerf 1994; Bono *et al.* 1998).
- Nonlinear effects such as the coupling between convection and pulsation, the convective overshooting and the superadiabatic gradients are fully taken into account.
- As for the opacity, which is a key ingredient for constructing stellar envelope models, we adopted OPAL opacities (Iglesias & Rogers 1996) for $T > 10,000$ K and molecular opacities (Alexander & Ferguson 1994) $T < 10,000$ K. The method adopted for handling opacity tables was discussed in Bono *et al.* (1996).
- Artificial viscosity was included following Stellingwerf (1975) prescriptions.
- To provide accurate predictions on the limit cycle behaviour of these objects, the gov-

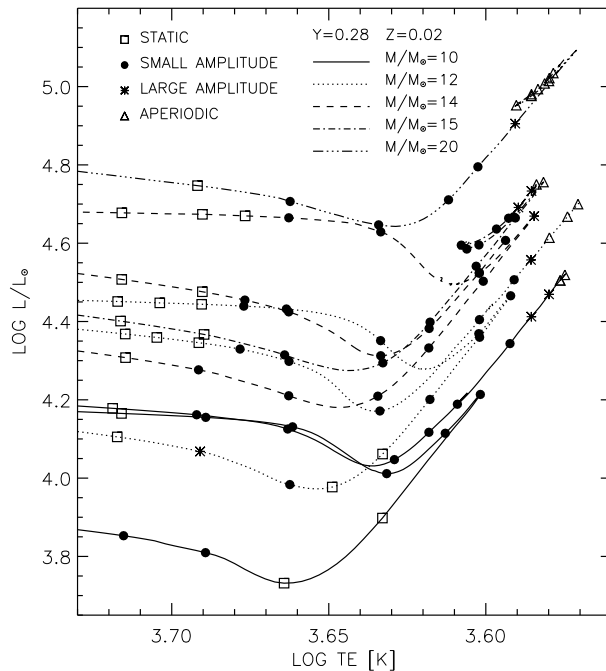


FIGURE 5. Evolutionary tracks and pulsation models at solar chemical composition in the HR diagram. Evolutionary models constructed by adopting different stellar masses are plotted by using different line styles, while pulsation models characterized by different limiting amplitude behaviours are plotted using different symbols. See text for further details.

erning equations were integrated in time for a number of periods ranging from 1000 to 5000.

In order to make a detailed analysis of RSG pulsation properties during both H and He burning phases, to be compared with actual properties of real RGS stars, we constructed several sequences of models at fixed chemical composition ($Y=0.28$, $Z=0.02$) which cover a wide range of stellar masses $10 \leq M_{\odot} \leq 20$. Moreover, since we are interested in mapping the properties of RSG stars from H-shell burning up to the central He exhaustion, both the luminosities and the effective temperature values were selected directly along the evolutionary tracks (see Figure 4). The evolutionary calculations were performed at fixed mass – *i.e.* no mass-loss – and neglecting the effects of both convective core overshooting and rotation. Since the pulsational properties of a star depend mostly on the physical structure of the envelope regions in which H and He undergo partial ionization, *i.e.* well above the layers in which the nuclear burning takes place, the use of constant mass evolutionary tracks for our study does not limit the qualitative value of our conclusions. However, self-consistent evolutionary models which properly include a parametrization of mass loss will eventually be needed for a full, quantitative description of the phenomenon (see Section 4).

The input physics and physical assumptions adopted for constructing evolutionary and pulsational models will be described in detail in a forthcoming paper (Bono & Panagia 2000). Figure 5 shows the location in the HR diagram of both evolutionary tracks and pulsation models we constructed. The pulsation models characterized by different limiting amplitude behaviour are plotted with different symbols. The squares refer to models

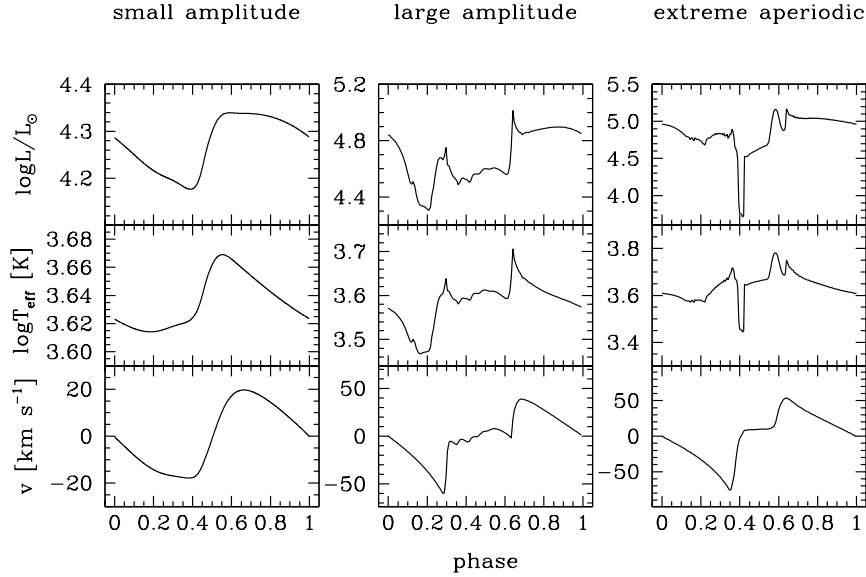


FIGURE 6. The cycle variation of luminosity, temperature and velocity for a $15 M_{\odot}$ red supergiant for three distinct regimes, small amplitude (left panel), large amplitude (central panel), and aperiodic extreme pulsations (right panel).

which are pulsationally stable, *i.e.* those in which, after the initial perturbation, the radial motions decay and the structure approaches once again the static configuration. Filled circles and asterisks refer to models which show small ($\Delta \log L < 0.4$) and large ($\Delta \log L > 0.4$) pulsation amplitudes together with a periodic behaviour (stable limit cycle). Triangles denote the models which not only present large pulsation amplitudes but also aperiodic radial displacements (unstable limit cycle). The behaviour of pulsation properties discloses several interesting features:

- 1) For effective temperatures lower than approximately 5100 K high-mass models are, with few exceptions, pulsationally unstable in the fundamental mode both during H shell and He burning phases.
- 2) The pulsational behaviour is mainly governed by the effective temperature and to a less extent by the luminosity. In fact, the transition from small to large pulsation amplitudes ($T_e \approx 3900$ K) and from periodic to aperiodic behaviour ($T_e \leq 3800$ K) take place roughly at constant temperature.
- 3) Current models support the evidence suggested by Li & Gong (1994) on the basis of linear, nonadiabatic models that RSG variables are pulsating in the fundamental mode. In fact we find that throughout this region of the HR diagram the fundamental mode is pulsationally unstable, whereas the first overtone is stable.
- 4) The region in which the models attain small amplitudes is the natural extension of the classical Cepheid instability strip. This confirms the empirical evidence originally brought out by Eichendorf & Reipurth (1979) and more recently by Kienzle et al. (1998), as well as the theoretical prediction by Soukup & Cox (1996).
- 5) Interestingly enough, theoretical light curves of periodic large amplitude models show

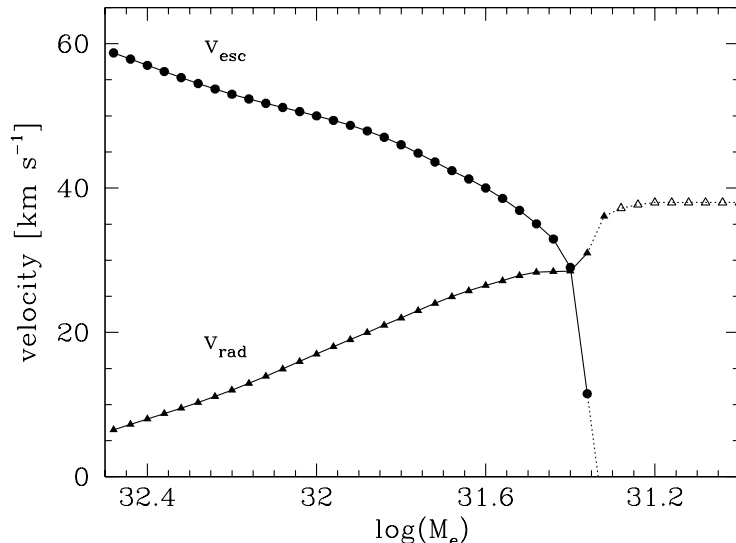


FIGURE 7. Radial velocity and escape velocity as a function of the mass as measured from the stellar surface for a $15 M_{\odot}$ star at $T_{eff}=3836$ K and $\log(L/L_{\odot})=4.75$.

the characteristic RV Tauri behaviour, i.e. alternating deep and shallow minima, observed in some RSG variables (Eichendorf & Reipurth (1979)).

3. Pulsationally Induced Mass Loss

As discussed above, in the reddest part of their RSG evolution, massive stars are found to pulsate with large amplitudes in both luminosity and velocity. In these phases, the radial velocity near the stellar surface may reach values of 50 km s^{-1} or higher, which may become higher than the effective escape velocity, *i.e.* the one computed by including both inward gravitational force and outward radiation acceleration. Therefore, the outer layers may become unbound and be lost from the system, thus producing a high mass loss rate. As an illustration, Figure 6 shows the variation of luminosity, temperature and velocity for a $15 M_{\odot}$ red supergiant for three distinct regimes, small amplitude (left panel), large amplitude (central panel), and aperiodic extreme pulsations (right panel).

In order to calculate pulsation induced mass loss, for each model we identify the outer layers for which

$$v_{rad} > v_{esc} + c_s$$

where v_{rad} is the radial velocity of a given layer, v_{esc} is the effective escape velocity that includes the effects of radiation forces, and c_s is the sound speed (Hill & Willson 1979). Those layers are effectively unbound and, therefore, are lost from the star. An example is shown in Figure 7 where we plot the actual velocity of the stellar envelope layers as a function of the stellar radius and compare them with the effective escape velocity. The mass present above the radius where the the actual velocity exceeds the escape velocity represents the amount of mass which is lost in a pseudo-impulsive event.

The characteristic time between successive pseudo-impulsive events is the Kelvin-Helmoltz time, *i.e.*

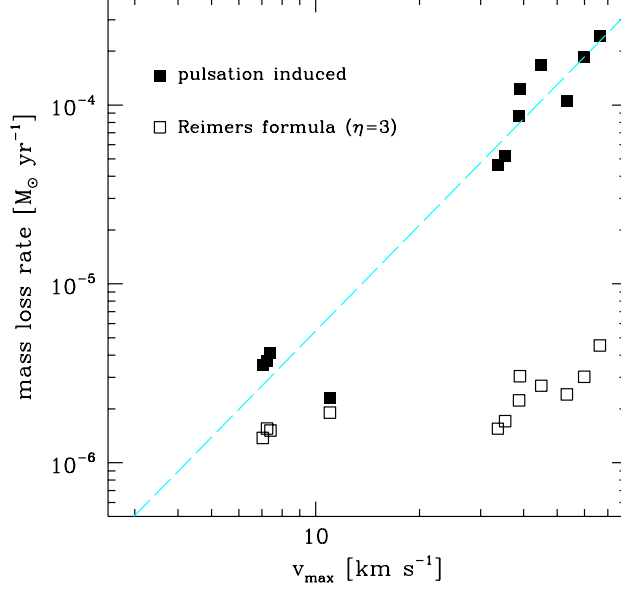


FIGURE 8. Mass loss rates as a function of the maximum velocity (see text). Filled symbols represent the pulsation-induced mass loss rates, and the open symbols the rates computed with Reimers' formula. The dashed line is a linear best-fit to the pulsation induced mass loss rates.

$$\tau_{KH} \simeq \frac{GM^2}{RL} = 63 \left[\frac{M}{10M_{\odot}} \right]^2 \left[\frac{R}{500R_{\odot}} \right]^{-1} \left[\frac{L}{10^5 L_{\odot}} \right]^{-1} \text{ yrs}$$

Thus, the mass loss rate is given by

$$\dot{M} = \frac{M(v > v_{esc} + c_s)}{\tau_{KH}}$$

An inspection to Figure 7 shows that layers as massive as $10^{-2} M_{\odot}$ may become unbound and be lost from the stellar surface within time intervals of several tens of years, thus producing mass loss rates of the order of several $10^{-4} M_{\odot} \text{ yr}^{-1}$ or even higher.

Following this recipe, we have determined the mass loss rates for several values of the stellar mass and for a variety of locations in the HR diagram. As shown in Figure 8, we find that the pulsation induced mass loss can satisfactorily be represented as a power law function of the maximum expansion pulsational velocity (*i.e.* the maximum velocity that is attained by the outermost layers in a pulsational cycle), *i.e.*

$$\log(\dot{M}) = -7.24 + 1.97 \times \log(v_{max})$$

Since pulsation-induced mass loss is an additional mass loss mechanism that comes on top of more conventional radiation-pressure induced mass loss, the total mass loss rate is assumed to be the straight sum of the two rates.

The main result is that including the effects of pulsations, the predicted mass loss rate in the RGS phase is a strong function of both the luminosity and the tempera-

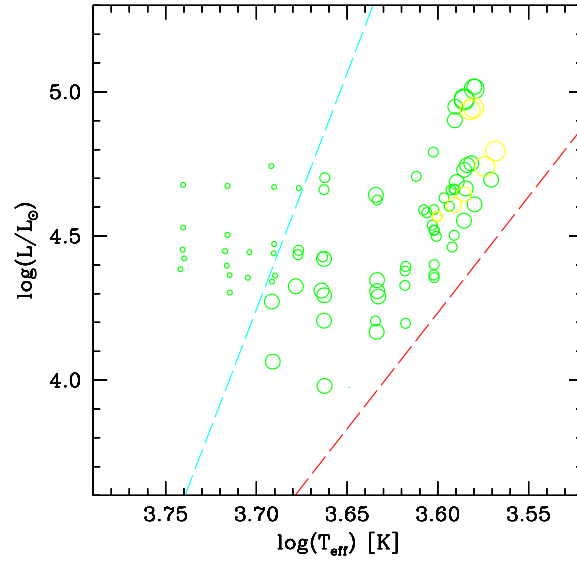


FIGURE 9. Pulsationally enhanced mass loss rates as a function of the position in the HR diagram. The size of the circles are proportional to the logarithm of the mass loss rate up to a maximum value of almost $10^{-3} M_{\odot} yr^{-1}$. Note the strong enhancement of the mass loss rate within the Cepheid instability strip (area within the dashed lines; Bono *et al.* 2000a).

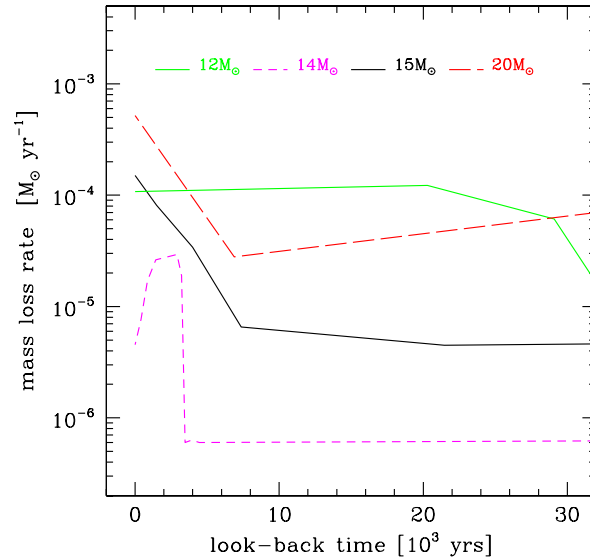


FIGURE 10. Pulsationally enhanced mass loss rates as a function of look-back time (short time-scale variation).

ture, in the sense that the mass loss process is strongly enhanced by pulsations when a star is moving toward cooler effective temperatures. Figure 9 illustrates this result and shows that now it should only take small adjustment to fully reproduce the observations. Moreover, since a red supergiant may cross the instability strip rather quickly, its mass loss can change considerably on relatively short time scales, thus accounting for another observational fact. It is worth mentioning that Feast (1991) found, on the basis of IRAS data for 16 RSG variables in the LMC, a period-mass loss relation. This relation supports a similar behaviour i.e. a steady increase in the mass-loss when moving from short to long period variables.

4. Discussion and Conclusions

The computed mass loss rates, for stars in the range 12-20 M_{\odot} , as a function of look-back time are displayed in Figures 10-12 for short (0-30,000 years), medium (0-150,000 years) and long time-scales (0-1 Myrs), respectively. We see that the mass loss rates may be as high as almost $10^{-3} M_{\odot} yr^{-1}$, i.e. similar to what is measured for extreme red supergiants, and may vary by an order of magnitude over relatively short times, say, 10,000 years or less. In other words the predicted mass loss rates are able to account, at least qualitatively, for all of the features observed in radio supernovae. Moreover, since the predicted mass loss history is a critical function of how a massive star evolves within the pulsation instability strip, a comparison between observations and theory should lead to an accurate determination of the stellar progenitor mass. For example, the mass loss decline of a 20 M_{\odot} star may be used to represent the apparent drop of emission of SN 1988Z about 9 years after explosion (cf. Figure 1). Similarly, the quick increase found for our 14 M_{\odot} model closely resembles the behaviour observed for SN 1993J. Of course, detailed comparisons will be meaningful only we will have a fully self-consistent set of evolutionary tracks (see below).

The mid- and long-term behaviour of the mass loss rate as a function of look-back time is also interesting because allows one to make predictions about the radio emission, as well as on *any* other phenomenon linked to a SN shock front and/or ejecta interaction with a dense circumstellar medium, such as relatively narrow optical emission lines and X-ray emission. As we can see in Figures 11 and 12, massive stars are expected to display rather sudden variations of their mass loss rates of all time scales, both because of pulsational instabilities which arise with crossing the instability strip (e.g. the 12 M_{\odot} star in the time range $20-60 \times 10^3$ years) and because of the so-called blue loops (an effect clearly apparent at look-back times around 0.4–1 Myrs) that are determined by a combination of core He-burning and shell H-burning (e.g. Brocato & Castellani 1993, Langer & Maeder 1995). Because of these effects, one may expect that in some cases, a SN may drop below detection limit for a while but still may have a renaissance, in the X-ray, optical and radio domains, several tens or hundreds of years later.

Also, we note in passing that our findings support the empirical evidence recently brought out by van Loon et al. (1999) on the basis of ISO data on RSG stars in the LMC. In fact, they found that the mass loss rates increase with increasing luminosities and decreasing effective temperatures and range from 10^{-6} up to $10^{-3} M_{\odot} yr^{-1}$. A strong dependence of the mass loss rate on the effective temperature in Tip-AGB stars was recently suggested by Schröder, Winters and Sedlmayer (1999) on the basis of theoretical evolutionary models which account for carbon-rich wind driven by radiation pressure on dust.

Another interesting consequence of our results is that a more efficient mass loss in the RSG phase implies a lower mass cutoff to produce Wolf-Rayet stars and, therefore,

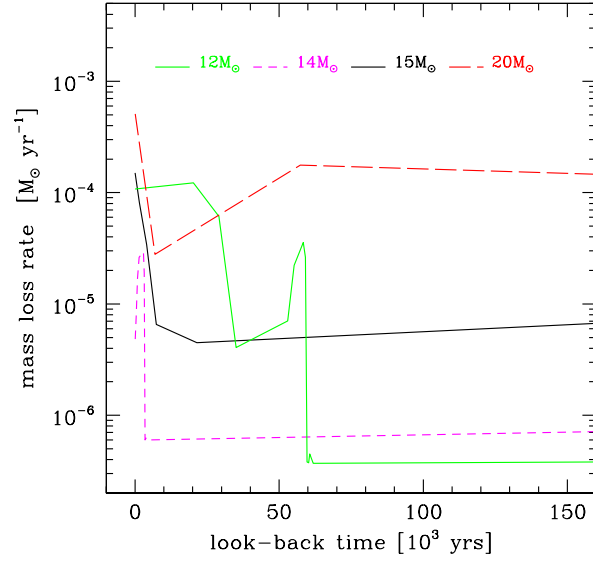


FIGURE 11. Pulsationally enhanced mass loss rates as a function of look-back time (medium time-scale variation).

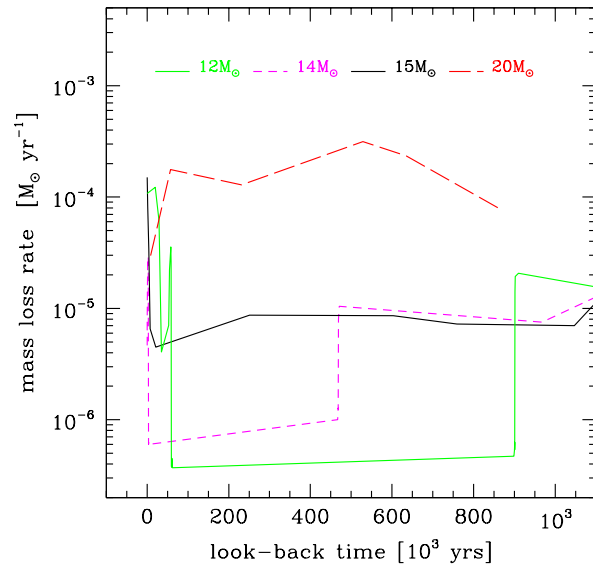


FIGURE 12. Pulsationally enhanced mass loss rates as a function of look-back time (long time-scale variation).

one has to expect a more efficient mass return into the ISM than commonly adopted in galactic evolution calculations.

Still there are improvements and refinements to apply to our models, because the calculations we presented here are not fully self-consistent in that we adopted evolutionary tracks computed either with no mass loss whatsoever, or with modest mass loss rates, and on them we performed our pulsational stability analysis and, thus, determined our new mass loss rates. Moreover, our models were constructed by adopting the diffusion approximation even in optically thin layers and therefore we neglected the dust formation processes (Arndt et al. 1997). A macroscopic example of the shortcomings of our current approach is that if we integrate the mass loss rates over time, in many cases we find that the star loses a substantial fraction of their mass before reaching its evolutionary end. Although this is close to what one should expect on the basis of observations, definitely it is at variance with the assumptions that went into the adopted evolutionary model calculations.

It is clear that what we need to do now is to follow an iterative procedure in which we first use our present prescriptions to compute new evolutionary tracks, then we repeat our pulsational stability analysis, then we compute new mass loss rates, and we iterate the procedure until adequate convergence is achieved. This work is in progress and will be presented in future papers. For the time being, our conclusions can be summarized as follow:

- We have defined a new theoretical scenario for pulsation induced mass loss in RSGs.
- RSGs are pulsationally unstable for a substantial portion of their lifetimes.
- Dynamical instabilities play a key role in driving mass loss.
- Bright, cool RSGs undergo mass loss at considerably higher rates than commonly adopted in stellar evolution.
- Comparisons of model predictions with observed CSM phenomena around SNII will provide valuable diagnostics about their progenitors and their evolutionary history.
- More efficient mass loss in the RSG phase implies a lower mass cutoff to produce Wolf-Rayet stars and a more efficient return of polluted material into the ISM, thus affecting the expected chemical evolution of galaxies.

REFERENCES

- ALEXANDER, D.R., & FERGUSON, J.W. 1994, *Astrophys. J.* **437**, 879
- ARNDT, T. U., FLEISCHER, A. J., & SEDLMAYER, E. 1997, *Astron. & Astrophys.* **327**, 614
- BENETTI, S., TURATTO, M., CAPPELLARO, E., DANZIGER, I. J., & MAZZALI, P. 1999, *Mon. Not. Roy. Astron. Soc.* **305**, 811
- BOFFI, F. R., & PANAGIA, N. 1996, in *Radio emission from the stars and the sun*, ASP Conference Series, Volume 93, ASP - San Francisco, p. 153-156
- BOFFI, F. R., & PANAGIA, N. 2000, in preparation.
- BONO, G., CAPUTO, F., CASSISI, S., MARCONI, M., & TORNAMBÈ, A. 2000b, *Astrophys. J.* submitted
- BONO, G., CAPUTO, F., & MARCONI, M. 1998, *Astrophys. J.* **497**, L43
- BONO, G., CASTELLANI, V., & MARCONI, M. 2000a, *Astrophys. J.* **529**, 293
- BONO, G., INCERPI, R., & MARCONI, M. 1996, *Astrophys. J.* **467**, L97
- BONO, G., MARCONI, M., & STELLINGWERF, R. F. 1999, *Astrophys. J. Suppl. Ser.* **122**, 167
- BONO, G., & PANAGIA, N. 2000, in preparation
- BONO, G., & STELLINGWERF, R. F. 1994, *Astrophys. J. Suppl. Ser.* **93**, 233
- BROCATO, E., & CASTELLANI, V. 1993, *Astrophys. J.* **410**, 99

- CHIEFFI, A., LIMONGI, M., & STRANIERO, O. 1998, *Astrophys. J.* **502**, 737
- CHU, Y.-H., CAULET, A., MONTES, M. J., PANAGIA, N., VAN DYK, S. D., & WEILER, K. W. 1999, *Astrophys. J.* **512**, L51
- CHUGAI, N.N., DANZIGER, I.J., & DELLA VALLE, M. 1995, *Mon. Not. Roy. Astron. Soc.* **276**, 530
- DE JAGER, C., NIEUWENHUIJZEN, H., & VAN DER HUUCHT, K.A. 1988 *Astron. & Astrophys. Suppl.* **72**, 295
- EICHENDORF, W., & REIPURTH, B. 1979, *Astron. & Astrophys.* **77**, 227
- FEAST, M. W. 1991, in *Instabilities in Evolved Super- and Hyper-Giants*, eds. C. de Jager & H. Nieuwenhuijzen, Amsterdam: North Holland, p. 18-21
- FOX, M. W., & WOOD, P. R. 1982, *Astrophys. J.* **259**, 198
- HEBER, A., JEANNIN, L., LANGER, N., & BARAFFE, I. 1997, *Astron. & Astrophys.* **327**, 224
- HILL, S. J., & WILLSON, L. A. 1979, *Astrophys. J.* **229**, 1029
- IGLESIAS, C. A., ROGERS, F. J. 1996, *Astrophys. J.* **464**, 943
- KIENZLE, F., BURKI, G., BURNET, M., & MEYNET, G. 1998, *Astron. & Astrophys.* **337**, 7 79
- LACEY, C., WEILER, K. W., SRAMEK, R. A., PANAGIA, N., & VAN DYK, S. D. 2000, in preparation
- LANGER, N., & MAEDER, A. 1995, **295**, 685
- LI, Y., & GONG, Z. G. 1994, *Astron. & Astrophys.* 289, 449
- MONTES, M. J., VAN DYK, S. D., WEILER, K. W., SRAMEK, R. A., & PANAGIA, N. 1998, *Astrophys. J.* **506**, 874
- MONTES, M. J., VAN DYK, S. D., WEILER, K. W., SRAMEK, R. A., & PANAGIA, N. 2000, *Astrophys. J.* in press
- PANAGIA, N., & LAIDLER, V.G. 1988, in *Supernova Shells and Their Birth Events*, ed. W. Kundt, Springer-Verlag, Berlin, p. 187-191
- REID, N., TINNEY, C., & MOULD, J. 1990, *Astrophys. J.* **348**, 98
- REIMERS, D. 1975, *Mém. Soc. Roy. Sci. Liège 6^e Ser.*, **8**, 369
- RYDER, S., STAVELEY-SMITH, L., DOPITA, M., PETRE, R., COLBERT, E., MALIN, D., & SCHLEGEL, E. 1993, *Astrophys. J.* **416**, 167
- SALAMANCA, I., CID-FERNANDES, R., TENORIO-TAGLE, G., TELLES, E., TERLEVICH, R.J., & MUNOZ-TUNON, C. 1998, *Mon. Not. Roy. Astron. Soc.* **300**, L17
- SALASNICH, B., BRESSAN, A., & CHIOSI, C. 1999, *Astron. & Astrophys.* **342**, 131
- SCHRÖDER, K. -P., WINTERS, J. M., & SEDLMAYER, E. 1999, *Astron. & Astrophys.* **349**, 898
- SOUKUP, M. S., & COX, A. N. 1996, *Astron. & Astrophys. Suppl.* **342**, 131
- STELLINGWERF, R. F. 1975, *Astrophys. J.* **195**, 441
- STELLINGWERF, R. F. 1982, *Astrophys. J.* **262**, 339
- STELLINGWERF, R. F. 1984, *Astrophys. J.* **284**, 712
- STOTHERS, R., & LEUNG, K. C. 1971, *Astron. & Astrophys.* **10**, 290
- VAN DYK, S. D., WEILER, K. W., SRAMEK, R. A., RUPEN, M., & PANAGIA, N. 1994, *Astrophys. J.* **432**, L115
- VAN LOON, J. TH., *et al.* 1999, *Astron. & Astrophys.* **351**, 559
- WOOD, P. R., *et al.* 1999, in IAU Symposium No. 191 *AGB Stars*, (San Francisco: ASP), in press